Exploiting nuclear duality of ciliates to analyse topological requirements for DNA replication and transcription

Jan Postberg[1,2,*], Olga Alexandrova[3], Thomas Cremer[2] and Hans J. Lipps[1]

[1]Institute of Cell Biology, University of Witten/Herdecke, Stockumer Str. 10, 58453 Witten, Germany
[2]Department Biology II, Anthropology and Human Genetics, Ludwig Maximilians University Munich, Großhaderner Str. 2, 82152 Martinsried, Germany
[3]Department Biology II, Cell and Developmental Biology, Ludwig Maximilians University Munich, Großhaderner Str. 2, 82152 Martinsried, Germany
*Author for correspondence (e-mail: janp@uni-wh.de)

Accepted 13 May 2005
Journal of Cell Science 118, 3973-3983 Published by The Company of Biologists 2005
doi:10.1242/jcs.02497

Summary

Spatial and temporal replication patterns are used to describe higher-order chromatin organisation from nuclei of early metazoan to mammalian cells. Here we demonstrate evolutionary conserved similarities and differences in replication patterns of micronuclei and macronuclei in the spirotrichous ciliate *Stylonychia lemnae*. Since this organism possesses two kinds of morphologically and functionally different nuclei in one cell, it provides an excellent model system to analyse topological requirements for DNA replication and transcription.

Replication in the heterochromatic micronucleus occurs in foci-like structures showing spatial and temporal patterns similar to nuclei of higher eukaryotes, demonstrating that these patterns are inherent features of nuclear architecture. The 'nanochromosomes' of the macronucleus are replicated in the propagating replication band. We show that it consists of hundreds of replication foci. Post-replicative macronuclear chromatin remains organised in foci. These foci are not randomly distributed throughout the macronucleus, indicating a higher-order organisation of macronuclear chromatin above the level of 'nanochromosomes'. Both telomerase and proliferating cell nuclear antigen (PCNA) occur as foci-like structures in the rear zone of the replication band, suggesting that a wave of chromatin modification driven by a short or continuous exogenous signal permits the assembly of replication factories at predicted sites. We further show that transcription occurs at discrete sites colocalised with putative nucleoli and dispersed chromatin.

Common principles of functional nuclear architecture were conserved during eukaryotic evolution. Moreover nuclear duality inherent to ciliates with their germline micronucleus and their somatic macronucleus may eventually provide further insight into epigenetic regulation of transcription, replication and nuclear differentiation.

Key words: Micronucleus, Macronucleus, Replication foci, Nuclear architecture, *Stylonychia lemnae*

Introduction

Research efforts over the last decades have shown that the eukaryotic cell nucleus has a compartmentalised structure with chromosome territories (CT) built up from chromatin domains with a DNA content of about ~1 Mbp and an interchromatin compartment (IC) (Cremer and Cremer, 2001; Cremer et al., 2004). Contrary to the impression given by textbooks that polymerases track along their templates like locomotives, nuclear processes such as the replication of DNA or transcription occur at specific sites (Cook, 1999), possibly in perichromatin regions at borders between chromatin domains and the interchromatin compartment (Jaunin and Fakan, 2002; Jaunin et al., 2000). The incorporation of halogenated nucleotides during S phase allowed the visualisation of these chromatin domains as so-called replication foci (Nakamura et al., 1986) in a wide range of evolutionary distant metazoan species and cell types, including cells from mammals, birds and *Hydra vulgaris* (Alexandrova et al., 2003; Habermann et al., 2001; Sadoni et al., 1999). Five patterns that are characteristic for successive stages of S phase were distinguished (O'Keefe et al., 1992). Briefly, pattern 1 is characterised by early-replicating foci scattered throughout the interior of the nucleus, specifically in regions of euchromatin, while the peripheral heterochromatin and some regions of the internal nucleoplasm are devoid of replication sites. Pattern 2 shows sites of replication localised at the nuclear periphery with fewer interior sites. Pattern 3 reveals sites of replication restricted to the nuclear periphery and to perinucleolar regions. Pattern 4 is defined by sites of DNA replication that have become larger in size and fewer in number. Sites are distributed throughout the nuclear interior with only a few discrete sites at the nuclear periphery. Pattern 5 is noted towards the end of S phase. At this stage smaller foci are associated with peripheral heterochromatin and fewer, larger foci with heterochromatin located in the nuclear interior. Remarkably, the definition of different replication-labelling patterns during S phase is to some extent arbitrary, because they reflect stages of a continuous process. Other

authors have chosen a simplified scheme and distinguished only early (reflecting patterns 1 and 2), mid- (pattern 3) and late (patterns 4 and 5) stages of S phase (Leonhardt et al., 2000). Notably, replication foci labelled during S phase persist as chromatin domains of approximately 1 Mbp during other stages of the cell cycle and in subsequent cell generations, as well as in post-mitotic cells (Sadoni et al., 2004), and may represent a fundamental structure of higher-order chromatin organisation in evolutionary distant species.

Although the spatial and temporal replication patterns described above demonstrate evolutionary conserved patterns of higher-order chromatin arrangements in all metazoa studied so far, only little is known about the nuclear architecture of replication and transcription in single-cell eukaryotes apart from yeast (Gasser, 2002; Pasero et al., 1999). Yeast cells, however, normally lack a thymidine kinase gene, and thus are usually not able to incorporate nucleoside analogues (Grivell and Jackson, 1968; Hodson et al., 2003). In contrast to yeast, but consistent with mammalian cells, spirotrichous ciliates were shown to incorporate nucleoside analogues efficiently (Ammermann, 1971; Olins and Olins, 1994; Prescott, 1994). These ciliated protozoan cells therefore easily permit single-cell analysis of replication patterns and timing. The spirotrichous freshwater ciliate *Stylonychia lemnae*, like other ciliated protozoa, possesses two morphologically and functionally different types of nuclei in one cell: the diploid germline micronucleus, which is transcriptionally inert, and the transcriptionally very active macronucleus. This species provides an excellent system to study higher-order chromatin arrangements in two types of nuclei within the same cell environment, which fulfil very different somatic and generative tasks. Fundamental components of the replication machinery are already well characterised. *Stylonychia* has previously been used to examine the nuclear organisation of telomeric complexes and the end-replication machinery (Jonsson et al., 2002; Jonsson, 2002; Mollenbeck et al., 2003; Postberg et al., 2001). For these reasons *Stylonychia lemnae* was used in the present study to elucidate whether spatial and temporal replication patterns typical for nuclei of metazoan cells have evolved already in single-cell eukaryotes. During vegetative growth micronuclei divide by conventional mitosis. Macronuclei undergo a process called amitosis, during which the nucleus divides and each daughter nucleus obtains roughly, but not necessarily, the same amount of DNA. A new macronucleus derives from a micronucleus when two cells of different mating types are mixed and sexual reproduction takes place. During this process, which is called conjugation, the old macronucleus degenerates (Ammermann et al., 1974). In the course of macronuclear differentiation, extraordinary DNA-reorganisation and DNA-elimination processes take place, resulting in a macronucleus with a genome that is highly reduced in complexity compared with the micronuclear genome (Ammermann et al., 1974; Kraut et al., 1986). The macronuclear DNA of *Stylonychia* consists of highly amplified, gene-sized DNA-molecules ranging from 0.4-20 kbp, each of which is terminated with telomeres (Kraut et al., 1986). Since these gene-sized DNA molecules show typical chromosomal features (i.e. telomeres and, most probably, origins of replication), these segments have occasionally been referred to as ‘nanochromosomes’ (Cavalcanti et al., 2004). *Stylonychia* possesses two micronuclei and one elongated macronucleus. Two ovoid distal parts of the macronucleus are linked by a thin connection. The existence of a macronuclear replication band was probably first observed in light-microscopy studies by Friedrich Stein in 1859 (Stein, 1859) and represents another characteristic feature of spirotrichs. Replication in the macronucleus of *Stylonychia* starts simultaneously at the two distal ends. Two replication bands migrate towards the thin connection between the two ovoid parts and disappear when S phase is finished. Electron-microscopy studies revealed that the replication band can be distinguished into two segments. The forward zone consists of regular chromatin fibres about 50 nm in diameter. These fibres disperse at the junction with the rear zone that contains fibres of about 10 nm in diameter. Condensed chromatin reappears at the distal end of the rear zone (Olins et al., 1981; Olins and Olins, 1994; Prescott, 1994). Using a gentle fixation method to preserve the 3D structure of the macronuclei and micronuclei we performed the following experiments. First, we studied the incorporation of halogenated nucleotides into newly synthesised DNA in the replication band of macronuclei. To characterise the spatial organisation and dynamics of the replication machinery in macronuclei, we investigated the localisation of telomerase because it is supposedly involved in the initiation of replication in ciliates and is therefore a major component of the replication machinery in these cells (Allen et al., 1985; Blackburn, 1991a; Blackburn, 1991b; Murti and Prescott, 1983). Additionally, the localisation of the processivity factor of polymerase δ, proliferating cell nuclear antigen (PCNA) was examined because PCNA occurs in the replication band and in micronuclei of the ciliate *Euplotes eurystomus* (Olins et al., 1989). Eukaryotic PCNA is a homotrimeric ring that encircles the DNA and is thought to act as a central loading-platform for a number of proteins involved in DNA replication and the duplication of epigenetic information (Gulbis et al., 1996; Krishna et al., 1994; Schurtenberger et al., 1998). Second, based on pulse-chase-pulse labelling with 5-iodo-2′-deoxyuridine (IdU) and 5-chloro-2′-deoxyuridine (CldU), we analysed the temporal and spatial replication patterns in the transcriptionally silent and the heterochromatic micronuclei of *Stylonychia*. Third, we investigated whether transcription takes place throughout the whole macronucleus or whether it is restricted to distinct functional domains. For transcription labelling, newly synthesised RNA of *Stylonychia lemnae* macronuclei was pulse-labelled with 5-fluorouridine (FU).

Our findings imply that both the higher-order organisation of replication and the topology of transcription in the nuclear apparatus of spirotrichous ciliates and also in nuclei of mammalian species share evolutionary conserved features.

Materials and Methods

Growth and synchronisation of *Stylonychia* and isolation of nuclei

Stylonychia lemnae were grown in Pringsheim medium (0.11 mM Na_2HPO_4, 0.08 mM $MgSO_4$, 0.85 mM $Ca(NO_3)_2$, 0.35 mM KCl, pH 7.0) and synchronised. Nuclei were isolated as described elsewhere (Ammermann et al., 1974; Juranek et al., 2000). Isolated nuclei were fixed in 2% paraformaldehyde for 20 minutes at room temperature, washed twice with PBS and immobilised on poly-L-lysine coated coverslips.

Replication-labelling

For replication-labelling, synchronised *Stylonychia* were incubated in Pringsheim medium containing 5-bromo-2′-deoxyuridine (BrdU), 5-iodo-2′-deoxyuridine (IdU) or 5-chloro-2′-deoxyuridine (CldU). For single-pulse labelling, *Stylonychia* were incubated in 250 μM BrdU for 45 minutes. For double-pulse labelling, *Stylonychia* were sequentially incubated with 250 μM IdU and 250 μM CldU. Between the pulses, intermediate chase-intervals of 2 or 4 hours were performed. Subsequently, nuclei were isolated, fixed and immobilised as described above.

Transcription-labelling

For pulse-labelling of newly synthesised RNA, synchronised *Stylonychia* were incubated in Pringsheim medium containing 5 mM 5-fluorouridine (FU) for 1 hour. Subsequently, nuclei were isolated, fixed and immobilised as described above.

Immunodetection of halogenated thymidine analogues

Nuclei were permeabilised with 0.5% Triton X-100–PBS for 20 minutes, followed by incubation with 0.1 M HCl for 5 minutes at room temperature. For DNA denaturation, nuclei were treated with 70% formamide in 2×SSC pH 7.4 (1×SSC is 0.15 M NaCl and 0.015 M Na citrate) for 3 minutes at 72°C. Nuclei were then briefly washed in ice-cold 70% ethanol followed by 100% ethanol and finally in PBS for 5 minutes. Blocking was done in 3% BSA, 0.1% Triton X-100, PBS (blocking solution) for 20 minutes at room temperature. Antibodies were diluted in blocking solution. Between application of primary and secondary antibodies nuclei were washed in PBS for 20 minutes. Incubations with all antibodies were performed for 1.5 hours at 37°C. BrdU incorporation was detected with monoclonal mouse anti-BrdU antibody (Sigma, clone BU 33) followed by sheep anti-mouse Cy3 conjugate (Sigma). For detection of IdU and CldU, preparations were incubated sequentially: (1) monoclonal rat anti-BrdU antibodies detecting also CldU (Diagnostic International, clone BU 1/75); (2) goat anti-rat Cy3 conjugate (Amersham); (3) monoclonal mouse anti-BrdU antibody detecting also IdU (Becton Dickinson, clone B44); (4) goat anti-mouse Alexa Fluor 488™ conjugate (Molecular Probes). FU incorporation was detected with monoclonal mouse anti-BrdU antibody and then with goat anti-mouse Alexa Fluor 488™ conjugate (Molecular Probes). Nuclei were counterstained with 0.1 μg/ml 4′,6-diamidino-2-phenyl-indole (DAPI) (Sigma) and 1 μM To-Pro-3 (Molecular Probes) in PBS. Preparations were mounted in Vectashield antifade medium (Vector Laboratories) and sealed with nail varnish.

Immunodetection of PCNA

Synchronised S-phase nuclei were permeabilised, blocked and washed, and antibodies were diluted in blocking solution as described above. Between the application of primary and secondary antibodies, washing steps were performed in PBS for 20 minutes. Incubations with all antibodies were performed for 1.5 hours at 37°C. PCNA was detected with human anti-PCNA antibody (Immuno Concepts, Auto I.D. positive control serum) and then with goat anti-human Alexa Fluor 488™ conjugate (Molecular Probes). Nuclei were counterstained, preparations were mounted and sealed as described above.

Fluorescence in-situ hybridisation and detection of hybridised probes

Immunolocalisation of telomerase was performed by fluorescence in-situ hybridisation (FISH), simultaneously with two oligonucleotide probes (5′-CTTGACAGCGTTATAGCTGACGGATTTCCGCCG-3′ and 5′-GGAACCAGGCGAATTGCTCTCATTTTACGGT-3′) labelled at their 3′-ends with digoxigenin-dUTP directed against two regions adjacent to the template region of *Stylonychia lemnae* telomerase RNA. The telomerase-RNA probe mixture was dissolved in hybridisation buffer (0.9 M NaCl, 20 mM Tris·HCl, pH 7.2, 0.01% SDS). Macronuclei were isolated, fixed and immobilised as described above. Nuclei were permeabilised with 0.5% Triton X-100–PBS for 20 minutes, followed by incubation with 0.1 N HCl for 5 minutes at room temperature. DNA was denatured with 70% formamide in 2×SSC pH 7.4 and incubated for 3 minutes at 72°C. The probe was denatured separately in boiling water for (10-minute incubation), briefly chilled on ice and subsequently loaded onto a coverslip with immobilised nuclei. Hybridisation was performed overnight at 42°C followed by post-hybridisation washes in 2×SSC at 42°C and 0.1×SSC at 60°C. Blocking was done in blocking solution for 20 minutes at room temperature. Antibodies were diluted in blocking solution as described above. Between application of primary and secondary antibodies, washing steps were performed in PBS for a total of 20 minutes. All incubations with antibodies were sequentially performed for 1.5 hours at 37°C. Mouse anti-digoxigenin monoclonal antibody (Sigma) was used as primary layer, goat anti-mouse Alexa Fluor 488™ conjugate (Molecular Probes) was used as secondary layer. Nuclei were counterstained, preparations were mounted and sealed as described above.

Confocal microscopy

Nuclei were analysed by laser-scanning confocal-microscopy. Optical serial sections were taken with a Leica TCP SP confocal laser-scanning microscope (Leica Microsystems, Mannheim) equipped with an oil immersion PlanApochromat 100/1.4 NA lens. Fluorochromes were visualised by an argon laser (excitation: 488 nm for Alexa Fluor 488™ and 514 nm for Cy3) and with a helium-neon laser (excitation: 633 nm for To-Pro-3). Fluorochrome images were scanned sequentially to generate 8-bit greyscale images. Image resolution was 512×512 pixels with a pixel size of 195-49 nm, depending on the selected zoom factor. The axial distance between optical serial sections was 250 nm. To obtain an improved signal:noise ratio, each section image was averaged from four successive scans. The 8-bit greyscale single-channel images were overlaid to an RGB image assigning a false colour to each channel, and were then assembled into tables using open source software ImageJ (ImageJ 1.31v, Wayne Rasband, NIH) and Corel Photo Paint 10 software. Following the visualisation of halogenated thymidine-analogues and of DNA counterstaining, 3D reconstructions were performed by surface rendering using AMIRA software (Amira 3.1, TGS Europe). Colocalisation analysis of nascent RNA and chromatin domains was performed using IMARIS software (Imaris 4.1.0, Bitplane AG).

Results

Morphology of the micronucleus and the macronucleus

The morphology of macronuclei and micronuclei in *Stylonychia lemnae* was examined by confocal microscopy after chromatin had been stained with To-Pro-3. Fig. 1 provides a typical example and shows that *Stylonychia lemnae* possesses two micronuclei and one elongated macronucleus. To verify that no major changes of nuclear morphology occur during the isolation of nuclei or the fixation with paraformaldehyde, the morphology of nuclei in fixed and unfixed whole cells was examined after staining chromatin with To-Pro-3. No alterations of nuclear morphology were observed (data not shown). Isolated and fixed nuclei were used to account for background immunofluorescence and to avoid cytoplasmic autofluorescence. The diameter of the spherical micronuclei is 6-8 μm; the size of a mature macronucleus is typically

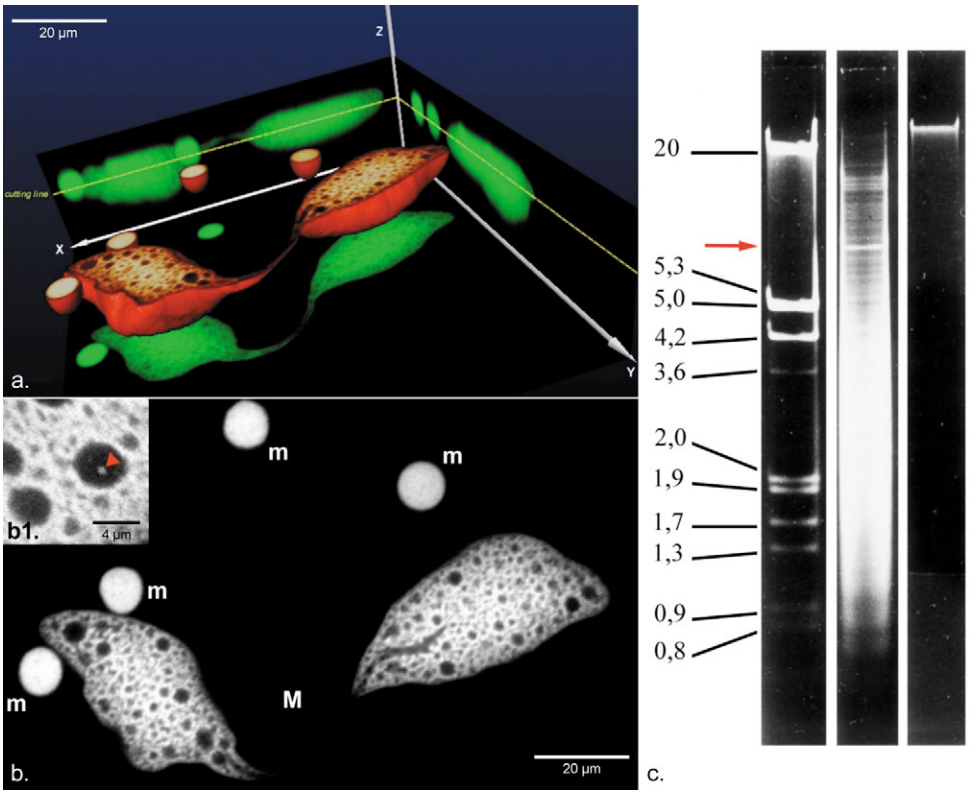

Fig. 1. Micronucleus and macronucleus morphology. View of four micronuclei and one macronucleus. To display the spherical organization of nuclei, a series of equidistant images (optical sections) were collected using laster-scanning-microscopy. (a) Average intensity planar projections (green) from a series of 42 optical sections were displayed onto planes between the *XY*-, *XZ*-, *YZ*-coordinate axes. 3D reconstruction (red) of the nuclear surface was rendered using To-Pro-3 counterstaining. The surface was partly cut to look inside, above the level of the yellow cutting line marked in planes *XZ* and *YZ*. (b) One optical section was selected from the middle of a series of equidistant images to display structural details of a macronucleus (M) and four micronuclei (m) stained with To-Pro-3. The nucleoplasmic connection between the ovoid distal parts of the macronucleus is not visible because it makes a turn, out of the single optical section. (Inset b1) Image taken from another mid optical section; magnification 2.5×. Red arrowhead indicates a central delimitated zone of stained chromatin within an unstained spherical putative nucleolus. (c) *Stylonychia lemnae* DNA on an agarose gel. Left, DNA size marker. Middle, macronuclear gene-sized DNA molecules of 0.4-20 Kbp. Arrow marks ribosomal DNA. Right, micronuclear DNA.

approximately 80-120 µm long and 25-40 µm wide. Two, more or less ovoid, distal parts of a macronucleus that often carry invaginations are linked by a thin nucleoplasmic connection (Figs 1a and 3a,c). Regions of highly condensed chromatin can be distinguished from regions with more dispersed chromatin (Fig. 1). The macronucleus contains numerous, mostly unstained, spherical structures with one or few delimitated spots of stained chromatin that is mostly located in the centre, or with no visible chromatin at all. These structures have been previously described as putative nucleoli (Kloetzel, 1970; Murti, 1973; Murti and Prescott, 2002) (Fig. 1b, inset b1). The macronuclear DNA of *Stylonychia* consists of about 15,000 different gene-sized molecules with of 0.4-20 kbp (Fig. 1c). Each of these 'nanochromosomes' is amplified to a copy number of several hundred to up to 10^6, and each is terminated with telomeres at both ends. By contrast, micronuclear DNA of *Stylonychia lemnae* is organised into approximately 120 chromosomes, each having an average size of 18 Mbp (Ammermann, 1970). The chromatin structure of its micronuclei appears very homogenous (Fig. 1b) and they possess no nucleoli (Prescott, 1994).

Topology of replication in the micronucleus

A question of outstanding interest is whether common principles of the nuclear topology of replication have been conserved in the eukaryotic lineage from ciliates to metazoa. We therefore investigated replication-labelling patterns during S phase of micronuclei. BrdU was incorporated into newly synthesised DNA in micronuclei of synchronised cells, followed by immunolocalisation of BrdU with fluorochrome-labelled antibodies. This approach demonstrated numerous discrete replication foci, scattered throughout the entire micronucleus. Foci appeared similar in size and shape, with a diameter of approximately 0.5 µm. To monitor temporal changes in the pattern of replication-foci, double-pulse-labelling with halogenated nucleotides (IdU, CldU) was performed (Fig. 2). Replication patterns in *Stylonychia* micronuclei revealed the same type 1 and type-2–type-3 patterns previously detected in nuclei of all metazoa studied so far (Fig. 2) (Alexandrova et al., 2003; Habermann et al., 2001; Sadoni et al., 1999). As micronuclei possess no nucleoli type 2 and type 3 patterns are indistinguishable in *Stylonychia* micronuclei. These experiments demonstrate that replication in the micronucleus occurs in foci-like structures with spatiotemporal patterns similar to higher eukaryotes. In nuclei of metazoan cells, transcriptionally active euchromatin typically replicates early during the first half of S phase, whereas transcriptionally silent heterochromatin replicates late during the second half of S phase (Stambrook and Flickinger, 1970). Since micronuclei are transcriptionally inactive and contain only heterochromatin, it can be concluded that the different topology of early and mid-late replicating chromatin is not causally related to differential transcriptional activity.

Organisation of the macronuclear replication band

Whereas the dynamic spatial order of replicating chromatin

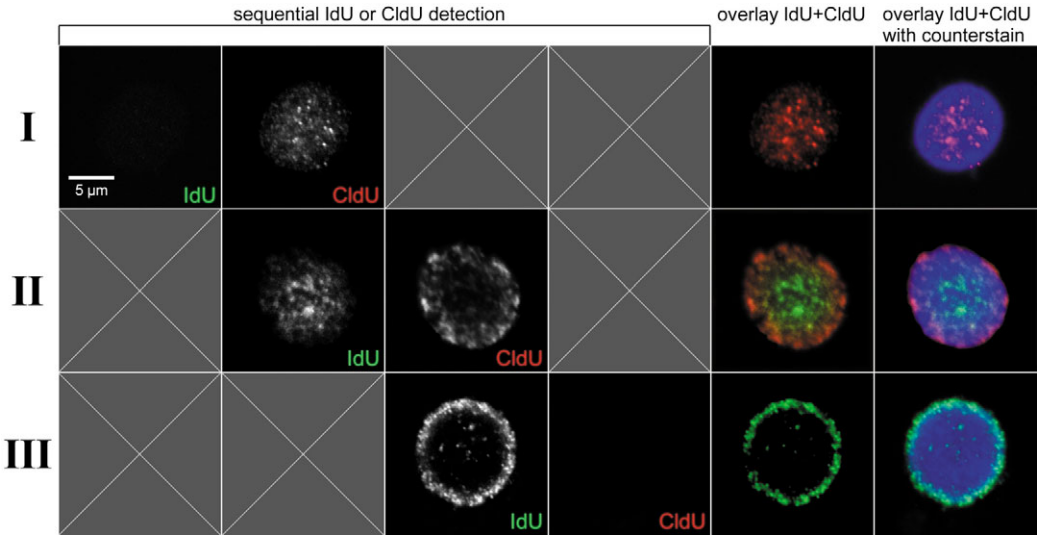

Fig. 2. Spatiotemporal replication patterns in micronuclei after pulse-chase-pulse labelling with IdU and CldU (pulse, 30 minutes; chase, 2 minutes; pulse, 30 minutes). Mid optical sections of three successive micronucleus replication stages. To-Pro-3 was used for counterstaining. Columns 1-4 (from left) show fluorochrome channels that had been scanned sequentially, generating 8-bit greyscale images. Columns 5 and 6, false colours were assigned to each channel (Alexa Fluor 488™, green; Cy3, red; To-Pro-3, blue) before being overlaid. Replication patterns resemble type 1 [I, CldU (red); II, IdU (green)] and type 2 and/or type 3 [II, CldU (red); III, IdU (green)].

patterns in micronuclei is consistent with the results of many previous studies of replication in metazoan species, the peculiar topology of DNA replication within a propagating, macronuclear replication band in spirotrichous ciliated protozoa offers an opportunity to study similarities and differences of this topology in a highly specialised nucleus (Fig. 3). In our experiments, the rear zone of the replication band was often identified in single optical sections with To-Pro-3 DNA counterstaining (Fig. 3a). The rear zone is the site of DNA synthesis and is built of chromatin fibers that are 10 nm in diameter (Evenson and Prescott, 1970; Lin and Prescott, 1985; Olins and Olins, 1994; Roth, 1957). To monitor sites of DNA replication in the macronucleus, BrdU was incorporated into newly synthesised DNA in S-phase macronuclei of synchronised cells; sites of DNA replication were then localised by immunofluorescence. Consistent with earlier autoradiographic analyses of [^{3}H]-thymidine incorporation into newly synthesised DNA in the *Euplotes* replication band (Olins

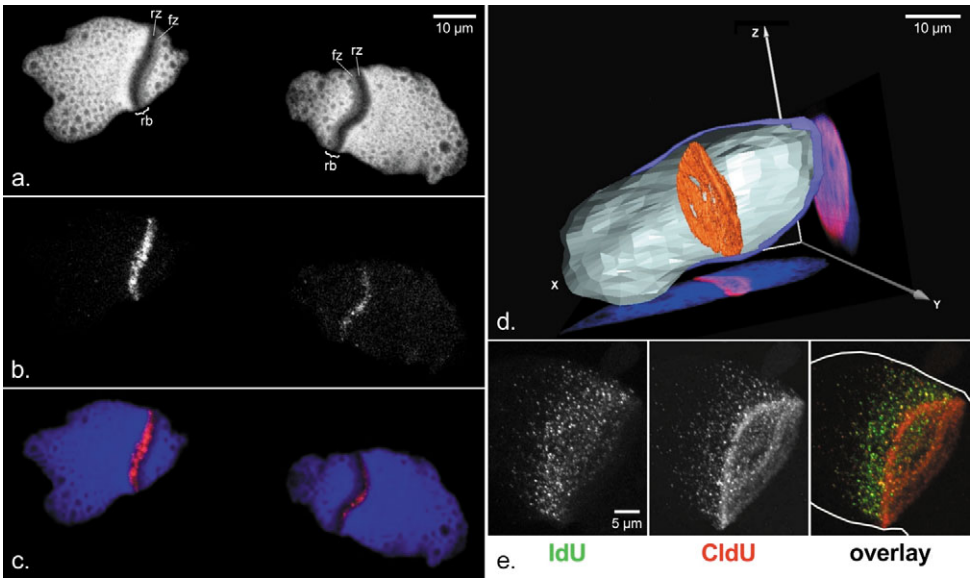

Fig. 3. The replication band of the macronucleus (rb, replication band; fz, forward zone; rz, rear zone). (a-c) Mid optical section of a macronucleus. a and b, Fluorochrome channels were scanned sequentially generating 8-bit greyscale images; a, To-Pro-3; b, BrdU pulse-labelling of replication foci (pulse 45 minutes) c, Overlay, with false colours assigned to each channel (To-Pro-3, blue; BrdU, red). (d) Average intensity projections (*XY* plane, *YZ* plane) of 63 serial optical sections. 3D reconstruction of the nuclear surface (blue) and the disc-shaped replication band (red). The surface was partly cut to look inside. (e) Sequential labelling of replication sites with IdU and CldU (pulse 30 minutes each, chase 5 minutes). Fluorochrome channels were scanned sequentially generating 8-bit greyscale images. Overlay with false colours assigned to each channel (IdU, green; CldU, red). Nuclear surface was rendered using To-Pro-3 counterstaining and marked by a white line in the overlay image. Sites of simultaneous IdU and CldU incorporation appear yellow. Replication occurs in hundreds of replication foci with a size of approximately 0.5 µm each. Initially, replication foci are more concentrated in the periphery (red). Later initiation of replication foci extends to the interior (yellow and green).

and Olins, 1994) the bulk part of BrdU-labelled nascent DNA colocalised with the rear zone of the replication band in *Stylonychia* (Fig. 3c). Fig. 3d presents a 3D reconstruction from a set of serial optical sections showing the disc-like organisation of the replication band. This disc spans through the entire transversal diameter of the macronucleus and is slightly thickened at its lateral boundaries. Earlier electron-microscopy studies reported that the shape of putative nucleoli does not change when passed by a replication band (Lin and Prescott, 1985). In the present study, we were unable to detect incorporation of BrdU within the spherical areas demarcated by putative nucleoli (data not shown). If these spherical structures were true nucleoli ribosomal genes should localise at such sites. That we were unable to detect BrdU incorporation in putative nucleoli could either mean that our present experiments lacked the sensitivity to detect the replication of ribosomal genes, or might be owing to the fact that the DNA encoding for ribosomal RNA was localised in the periphery of these structures and thus could not be distinguished from the bulk DNA. Alternatively ribosomal genes in putative nucleoli were possibly replicated independently from the propagating replication band and thus escaped detection when they underwent replication before or after passing the replication band. Since it has never unequivocally been demonstrated where ribosomal RNA synthesis takes place in macronuclei, putative nucleoli might in some or even all cases not represent true nucleoli, i.e. sites of ribosomal RNA synthesis. However, they might still play a role as sites of rRNA processing.

The replication band was assumed to reflect a huge, single replication factory (Prescott, 1994). This hypothesis is refuted by our experiments, because we observed that replication within the replication band occurs simultaneously in numerous discrete replication foci, each with a diameter of approximately 0.5 μm, i.e. the same size typically found for replication foci in nuclei of metazoan cells (Fig. 3b,c,e) (Hozak et al., 1994; Nakamura et al., 1986; O'Keefe et al., 1992). This means that replication in the replication band is a spatially and temporally highly synchronised event, with hundreds of single replication foci being activated simultaneously.

To distinguish replication foci on which replication was successively initiated in macronuclei during S phase, we performed pulse-chase-pulse labelling experiments with IdU and CldU. Initially, replication foci were concentrated in the peripheral area of the disc-shaped replication band, whereas

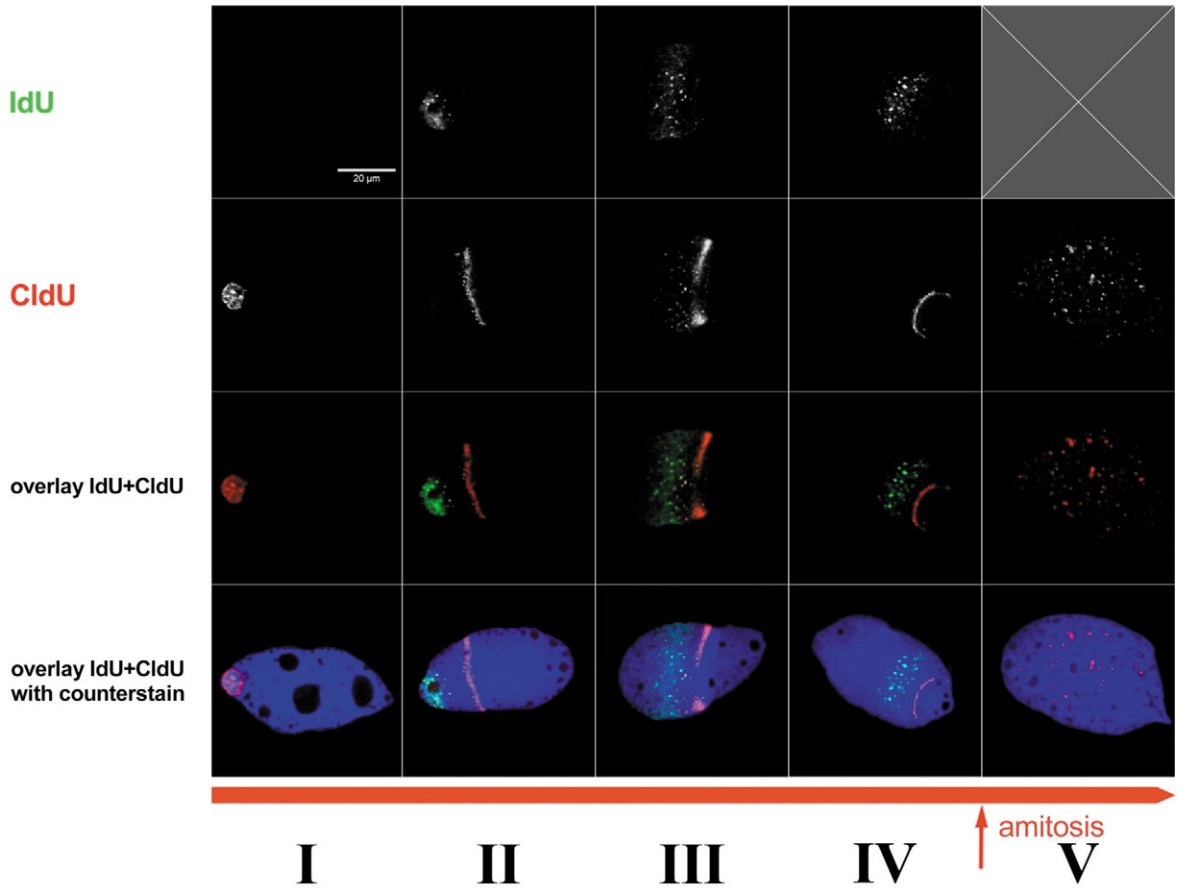

Fig. 4. Spatiotemporal replication patterns over the entire macronucleus S phase (approximately 6-8 hours). Mid optical sections of four macronuclei after pulse-chase-pulse labelling with IdU and CldU (pulse, 30 minutes; chase, 2 hours; pulse, 30 minutes) (I-IV) and of one macronucleus after pulse labelling with CldU followed by a 24-hour chase (V). Focal organisation of IdU-labelled post-replicative DNA is preserved even after a total chase of 2.5 hours (chase for 2 hours + second pulse for 30 minutes) or of 4.5 hours (chase for 4 hours + second pulse for 30 minutes; data not shown). These foci still appear as a dispersed band suggesting that mobility of post-replicative foci is strictly limited (II-IV). Focal organisation remains preserved even after amitosis (V), but foci are scattered throughout the entire volume of the macronucleus.

foci that had been initiated later extended more to the centre of the replication band (Fig. 3e).

To investigate potential movements of replication foci, we monitored the replication of macronuclear DNA over the entire S phase and after amitotic division. Between the two successive pulses with IdU and CldU, we allowed an extended chase of 2 hours. With a DNA content in *Stylonychia* macronuclei of 788 pg (Kraut et al., 1986) and S-phase duration of 6-8 hours, DNA polymerases replicate 1.7-2.2 pg of DNA per minute. Thus replication of even the largest gene-sized DNA molecules with of approximately 20 kbp must have been finished within a chase of 2 hours. Fig. 4I-III demonstrates that the localisation of replication foci, whose replication was initiated and completed during the first pulse (IdU, 30 minutes, green) became apparently more dispersed during the chase period when compared with the more compact and thinner replication band detected in nuclei fixed immediately after completion of the second pulse (CldU, 30 minutes, red). However, such post-replication foci still appeared as a band. Even after the chase period between two pulses was increased to four hours, post-replicative foci were localised within a dispersed disc-like area (data not shown). These results indicate that the mobility of replicated chromatin is constrained. In agreement with previous studies of nuclei from metazoan species, the focal chromatin structure was maintained after DNA replication had been completed, even in macronuclei following amitotic nuclear division. Notably, after the division of the macronucleus, the persistent chromatin domains – representing previously pulse-labelled replication foci – became scattered over the entire volume of the new macronucleus (Fig. 4V).

Assembly of telomerase and PCNA at replication foci in the macronucleus

To characterise the dynamics of the replication machinery, we investigated the localisation of PCNA. Also studied was the distribution of telomerase in the macronuclear replication band, because apparently it is also involved in the initiation of replication of the gene-sized DNA molecules either at or near telomeric ends (Allen et al., 1985; Blackburn, 1991a; Blackburn, 1991b; Murti and Prescott, 1983) as soon as such ends enter the rear zone from the forward zone (Prescott, 1994). We monitored the localisation of telomerase by FISH of telomerase RNA with digoxigenin-tailed oligonucleotide probes targeted to sequences adjacent to the template region (Fig. 5a-d). This experiment demonstrated the accumulation of telomerase in distinct foci-like structures in the replication band. Although these foci resembled replication foci in size and shape, we could not yet prove their correlation. Telomerase foci colocalised with the rear zone of the replication band, i.e. the zone where the incorporation of halogenated thymidine-analogues occurred, indicating that telomeric end-replication occurs in this zone. The temporal resolution of the present experiments, however, did not suffice to distinguish whether

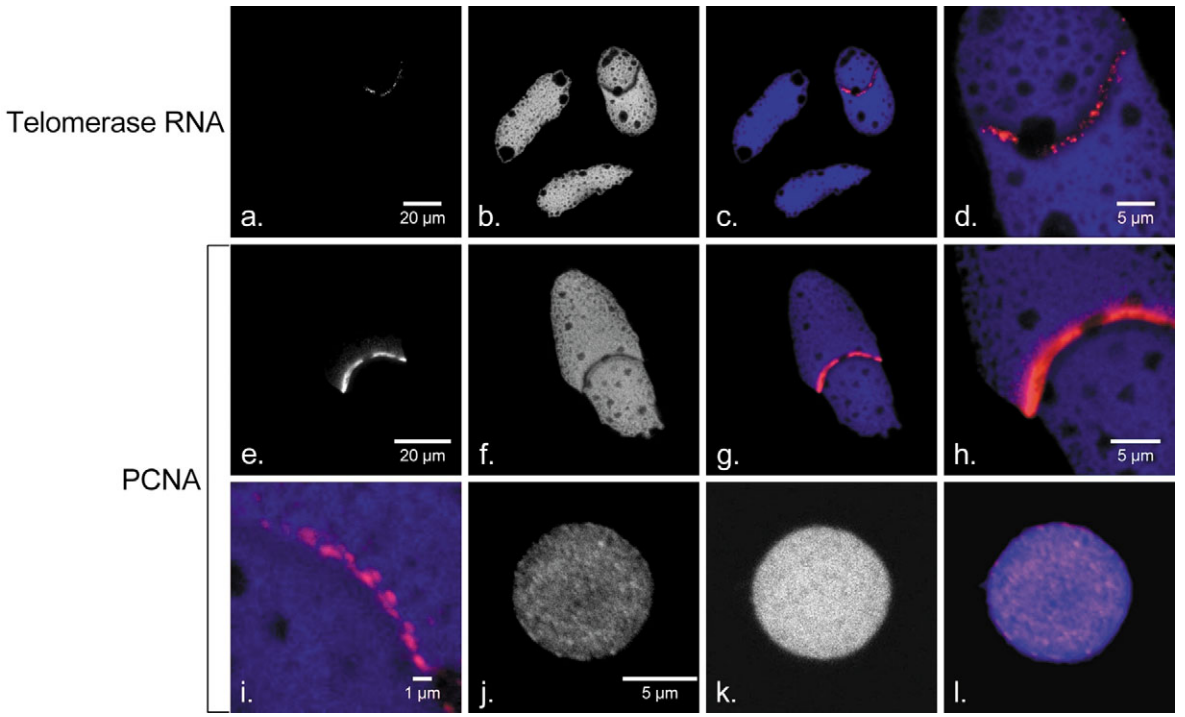

Fig. 5. Proteins associated to replication in *Stylonychia lemnae* macronuclei. Immunolocalisation of the (a-d) catalytic subunit of telomerase and of (e-f) PCNA. Accumulation of telomerase and PCNA in the replication band. Mid optical sections. (a-d) Immunolocalisation of the catalytic subunit of telomerase by FISH with probes against sequences adjacent to the template region of *Stylonychia lemnae* telomerase RNA. (a-c) Fluorochrome channels were scanned sequentially generating 8-bit greyscale images. (a) Telomerase RNA (red), (b) To-Pro-3 (blue). (c) Overlay, with false colours assigned to each channel. (d) Overlay; detailed view of a replication band from a-c. (magnification ×4). (e-l) Immunolocalisation of PCNA in (e-i) macronuclei and (j-l) one micronucleus. Fluorochrome channels were scanned sequentially generating 8-bit greyscale images. (g,h,i,l) Overlay, with false colours assigned to each channel, PCNA, red (e,j); To-Pro-3, blue (f,k). Detailed views of replication bands (h,i).

replication of the gene-sized DNA molecules in macronuclei is in fact initiated at telomeric ends. As described above for the incorporation of halogenated DNA-precursors, no telomerase was localised within the spherical area of putative nucleoli passed by a replication band (Fig. 5d). Consistent with earlier observations made in *Euplotes eurystomus* (Olins et al., 1989), immunolocalisation of PCNA revealed that this protein was also highly enriched within the replication band (Fig. 5e-l). We observed that PCNA occurs as foci, which were localised in the rear zone of the replication band (Fig. 5i). As expected, PCNA signals occurred as foci-like accumulations, distributed throughout the micronucleus (Fig. 5j-l).

Topology of transcription in the macronucleus

In the compartmentalised eukaryotic cell nucleus transcription occurs at specific sites, and it has been proposed that these sites are localised in perichromatin regions that border chromosome territories and the interchromatin compartment (Cremer and Cremer, 2001; Cremer et al., 2004). We asked whether a similar functional partition is adopted in the macronucleus of spirotrichs with its 'nanochromosomal' organisation. For pulse-labelling experiments 5-fluorouridine was incorporated into newly synthesised RNA (Boisvert et al., 2000). We monitored whether transcription takes place throughout the whole macronucleus in both condensed and dispersed chromatin regions or whether it is restricted to the latter. Whether transcription takes place within a passing replication band or whether it is restricted to nuclear areas outside the replication band was further examined. The results of these experiments suggest that transcription occurs preferentially within nuclear regions that contain dispersed chromatin and that it is excluded from more condensed chromatin. Furthermore, an association of nascent RNA with spots of stained chromatin in the centre of putative nucleoli was observed (Fig. 6). Colocalisation analysis of nascent RNA and DNA in serial optical sections of a macronucleus, yielded a negative correlation coefficient of r=–0.15 ±0.03, providing further evidence that transcription is excluded from regions of condensed chromatin. Within replication bands nascent RNA could not be detected, corroborating earlier observations that transcriptional activity is silenced in the replication band (Prescott and Kimball, 1961).

Discussion

Our study revealed striking similarities as well as differences in the higher-order chromatin architecture of micronuclei and macronuclei of *Stylonychia lemnae* when compared with each other and compared with nuclei of metazoan cells. *Stylonychia* provides an ideal model system, where the functional necessities of micronuclei, which solely serve a germline role, can be discriminated from macronuclei, which could be optimised during evolution for their role in gene regulation and transcriptional activities. Differences of higher-order chromatin structures in micronuclei and macronuclei provide

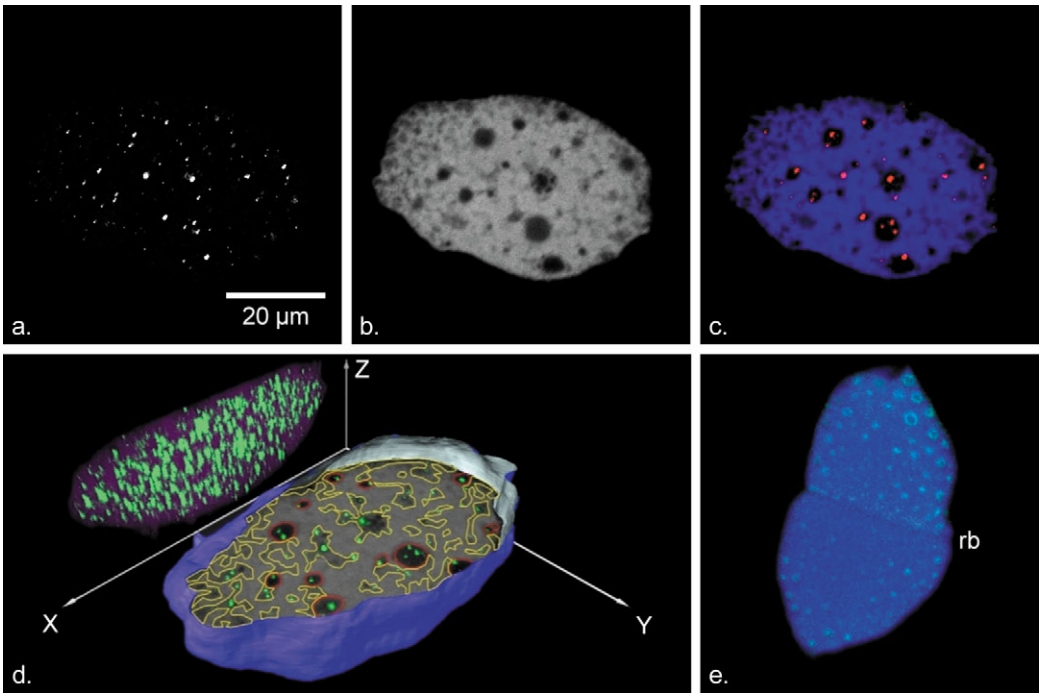

Fig. 6. (a-d) Immunolocalisation of nascent RNA after pulse labelling with FU and (e) total RNA staining with SYTO RNASelect in unfixed macronuclei. Transcription occurs in distinct foci colocalised with nucleoli and dispersed chromatin. Mid optical section of one macronucleus (a-c). Fluorochrome channels were scanned sequentially generating 8-bit greyscale images. (a) FU incorporated into newly synthesised RNA. (b) To-Pro-3. (c) Overlay, with false colours assigned to each channel (FU, red; To-Pro-3, blue). (d) Average intensity projection of 62 serial optical sections to a plane between *XZ*-coordinate axes and 3D reconstruction of the nuclear surface (blue) with one optical section. FU incorporated into newly synthesised RNA (green). Putative nucleoli are marked by a red line, domains of dispersed chromatin are marked by a yellow line. The surface was partly cut to look inside. (e) The rear zone of the replication band remains unstained when SYTO RNASelect is used as a RNA selective dye (green).

a possibility to distinguish structural peculiarities, which serve specific functional purposes. In contrast, the comparison of similarities in higher-order chromatin arrangements between micronuclei and macronuclei and nuclei from metazoan species helps to distinguish features, which serve functional needs common in all types of nuclei. Another phenomenon restricted to the macronucleus of spirotrichs is the simultaneous occurrence of the pre-replicative G1 stage in front of the replication band, the S-phase stage within this band and the post-replicative G2 stage behind the replication band.

Comparison of DNA replication topology in the micronucleus and macronucleus with nuclei of metazoa

Whereas the micronucleus is made up of about 120 chromosomes, with typical chromosomal organisation and an average DNA content of approximately 18 Mbp for each chromosome, the macronucleus contains gene-sized DNA molecules ranging from 0.4 to 20 kbp that are organised in nucleosomes (Lipps et al., 1978). Occasionally, these segments have been referred to as 'nanochromosomes', because each segment shows typical chromosomal features. These include telomeres at both ends and most probably an origin of replication. 'Nanochromosomes' lack, however, a centromere and are not faithfully propagated during amitosis to daughter nuclei. Pulse-labelling of micronuclei and macronuclei with halogenated thymidine-analogues revealed that replication occurred in replication foci, undistinguishable in diameter (~500 nm) and shape of replication foci of many metazoan species of both the animal and plant kingdoms (Alexandrova et al., 2003; Habermann et al., 2001; Hozak et al., 1994; Mayr et al., 2003; Nakamura et al., 1986; O'Keefe et al., 1992; Sadoni et al., 1999). In metazoan species, replication foci visualised by pulse-labelling experiments during S phase, contain approximately 1 Mbp of DNA and persist as distinct higher-order chromatin structures, termed ~1 Mbp-chromatin domains (Cremer and Cremer, 2001), at all stages of the cell cycle. Although we do not have quantitative measurements of the DNA content in replication foci of *Stylonychia*, it seems reasonable to assume that – based on similar fluorescence intensity of these foci and replication foci observed in other species – important features of the topological organisation of DNA replication have been evolutionarily conserved in both single-cell and multicelluar eukaryotes. Assuming a DNA content of approximately 1 Mbp for replication foci in macronuclei, we further conclude that 'nanochromosomes' form persistent higher-order chromatin structures in macronuclei.

When micronuclei were sequentially pulse-labelled with IdU followed by CldU during S phase, we observed replication patterns similar to type 1 and type 2-type 3. Initially, replication foci are scattered through the entire volume of the micronucleus but later, the peripheral localisation of replication foci is more pronounced. By definition, type 3 replication patterns reveal sites of replication restricted to the nuclear periphery and to perinucleolar regions. In *Stylonychia* micronuclei, type 3 patterns cannot be distinguished from type 2 patterns because these nuclei are transcriptionally inactive and possess no nucleoli. In general, transcriptionally active euchromatin replicates early during the first half of S phase, whereas transcriptionally silent heterochromatin replicates late during the second half of S phase (Stambrook and Flickinger, 1970). Since micronuclei are transcriptionally silent and exclusively contain homogenously stained constitutive heterochromatin, the similarity of the radial distribution of early and mid- to late replicating chromatin in micronuclei with transcriptionally active nuclei in metazoa allow the conclusion that this distribution is independent on chromatin activity and has evolved in single-cell eukaryotes. Moreover, it has probably been conserved since then in all typical eukaryotic nuclei as an intrinsic feature because of adaptive advantages, which are unrelated to transcription, splicing and RNA export.

Apart from the similarities of spatial patterns and in timing of replication, observed in micronuclei and nuclei of metazoan cells, the extremely localised and synchronised replication within the macronuclear replication band provides an excellent opportunity to characterise the dynamics of replication in eukaryotic cell nuclei. The replication bands characteristic for the macronuclei of spirotrichous ciliates have never been observed in any metazoan species. By means of pulse-chase-pulse experiments, with a short chase between the pulses of IdU and CldU, we found that initially replication sites were mostly concentrated at the periphery of the replication band, whereas later initiated sites preferentially localised in the centre of the replication band. This observation indicates that a directed replication-initiation wave starts at the lateral boundaries of the replication band and spreads to the interior. The propagation of this wave successively affects neighbouring foci, while individual foci apparently stay in place or, at most, show highly constrained local movements. Although further experiments with live ciliates are necessary for definite proof, our observations show a clear similarity to the 'domino effect model' of DNA replication proposed by Sporbert et al. (Sporbert et al., 2002).

At the same time the two replication bands propagate from distal macronucleus tips towards the thin connection between the two ovoid parts of a *Stylonychia* macronucleus. The peripheral parts of a replication band appear to propagate faster than the interior parts. As a consequence, the replication band gets more and more curved during later S phase. Even after an extended chase post-replicative chromatin foci or domains remained localised in a dispersed disc-shaped area, the former replication band. Whereas the structural reason for this constrained mobility of foci is not clear, this observation in itself, together with the apparent ~1 Mbp organisation of macronuclear replication foci, strongly suggests a higher-order organisation above the level of 'nanochromosomes'. The possibility of a higher-order organisation of 'nanochromosomes' is supported by electron-microscopy studies, which show that telomeres of the macronucleus interact end-to-end in the presence of increasing concentrations of monovalent ions (Lipps, 1980; Lipps et al., 1982). Recent studies further demonstrate that telomeric DNA bound by telomere end-binding proteins (TEBPs) interacts to form higher-order chromatin structures. It has been shown that anti-parallel G-quadruplex conformation could play an important role for the maintenance of telomeric complexes (Schaffitzel et al., 2001). These interactions are resolved in the replication band (Jonsson et al., 2002; Postberg et al., 2001). Other electron-microscopy studies showed that chromatin of the macronucleus forms rosette-like DNA-protein structures after

limited proteolysis (Murti and Prescott, 2002; Prescott, 1994). When *Stylonychia* macronuclei are examined in spread electron microscopical preparations, long continuous chromatin fibres can be visualised (Meyer and Lipps, 1981).

Notably, the foci-like organisation of replicated chromatin was preserved even after amitosis. After division of the macronucleus, however, replication foci were scattered over the entire volume of the new macronucleus. Referring to this observation, the reorganisation of the higher-order chromatin structure in macronuclei from one cell cycle to the next is consistent with a probabilistic nature of 'nanochromosome' arrangements. A probabilistic nature of chromosome neighbourhoods was also demonstrated for chromosome neighbourhoods in human cell nuclei (Bolzer et al., 2005).

Aside from spatial and temporal arrangements of replication foci in the macronucleus we were interested in the dynamics of the replication factories during the course of replication. High concentrations of telomerase or PCNA were detected in chromatin foci in the rear zone of the replication band, whereas in its front and behind of it no immunolocalisation was observed. From the fact that replication foci persist as organisational units after replication is accomplished and even from one cell division to the next, and from the observation that telomerase and PCNA assemble to replication foci exclusively when replication takes place during the macronucleus S phase, we conclude that the assembly of replication factories by a replication-competent chromatin domain is triggered by unknown modifications at the chromatin level. We assume that a wave of chromatin modifications driven by a short or a continuous exogenous signal permits the assembly of replication factories at predicted sites. The molecular nature of these modifications is presently not known.

Comparison of the topology of transcription in the macronucleus with nuclei of metazoa

The macronucleus shows domains of condensed and dispersed chromatin and possesses numerous putative nucleoli, containing one or few spots of stained chromatin similar to nucleolar fibrillar centres (FCs) of higher eukaryotes. Transcription apparently takes place within regions of dispersed chromatin. Owing to the limited resolution of the present study, we could not clearly distinguish in FU pulse-labelling experiments, whether the formation of nascent RNA occurred preferentially at border zones between regions of condensed and decondensed chromatin or on chromatin loops expanding from adjacent condensed chromatin regions into such zones. Whereas macronuclear zones in front and behind the replication band showed transcriptional activity, RNA pulse-labelling experiments did not show detectable amounts of nascent RNA within the replication band. The separation of condensed-chromatin regions from regions containing dispersed or no chromatin and also the topology of the transcription process reveals similarities to the higher-order chromatin organisation with interconnected zones of chromatin made from chromosome territories, and the interchromatin compartment previously described for nuclei of metazoan cells (Cremer and Cremer, 2001; Cremer et al., 2004). Our observations suggest the possibility that 3D networks of more condensed chromatin and an interchromatin compartment adjacent to this chromatin network can assemble in the absence of typical chromosomes. These data provide important hints that the topology of transcription in spirotrichous ciliate macronuclei and nuclei of mammalian species (Fakan and Van Driel, 2004) shows evolutionary conserved features. Further studies, including electron-microscopy investigations of transcription, are necessary to further test this hypothesis.

The last common ancestor of ciliates and mammals had lived in the later proterozoic of the precambrian era – i.e. at least 543 million years ago – as inferred from molecular data and fossil record of alveolates (including ciliates, dinoflagellates, foraminifera) (Erwin and Davidson, 2002; Javaux et al., 2003; Wray et al., 1995). Our results give striking support to the assumption that common organisational principles of functional nuclear architecture have been conserved during this long period of eukaryotic evolution. Moreover, the nuclear duality inherent to ciliated protozoan eukaryotes with their germline micronucleus and their transcriptionally active macronucleus allows a continuing and intriguing opportunity to provide insight into epigenetic regulation of transcription, replication and nuclear differentiation.

This work was supported by the Deutsche Forschungsgemeinschaft and the National Science Foundation (grant no: EIA-0121422). We thank Heiner Albiez and Irina Solovei for helping with bioinformatics and for fruitful discussions.

References

Alexandrova, O., Solovei, I., Cremer, T. and David, C. N. (2003). Replication labeling patterns and chromosome territories typical of mammalian nuclei are conserved in the early metazoan *Hydra*. *Chromosoma* **112**, 190-200.

Allen, R. L., Olins, A. L., Harp, J. M. and Olins, D. E. (1985). Isolation and characterization of chromatin replication bands and macronuclei from *Euplotes eurystomus*. *Eur. J. Cell Biol.* **39**, 217-223.

Ammermann, D. (1970). The micronucleus of the ciliate *Stylonychia mytilus*; its nucleic acid synthesis and its function. *Exp. Cell Res.* **61**, 6-12.

Ammermann, D. (1971). Morphology and development of the macronuclei of the ciliates *Stylonychia mytilus* and *Euplotes aediculatus*. *Chromosoma* **33**, 209-238.

Ammermann, D., Steinbruck, G., Berger, L. V. and Hennig, W. (1974). The development of the macronucleus in the ciliated protozoan *Stylonychia mytilus*. *Chromosoma* **45**, 401-429.

Blackburn, E. H. (1991a). Structure and function of telomeres. *Nature* **350**, 569-573.

Blackburn, E. H. (1991b). Telomeres. *Trends Biochem. Sci.* **16**, 378-381.

Boisvert, F. M., Hendzel, M. J. and Bazett-Jones, D. P. (2000). Promyelocytic leukemia (PML) nuclear bodies are protein structures that do not accumulate RNA. *J. Cell Biol.* **148**, 283-292.

Bolzer, A., Kreth, G., Solovei, I., Koehler, D., Saracoglu, K., Fauth, C., Muller, S., Eils, R., Cremer, C., Speicher, M. R. et al. (2005). Three-dimensional maps of all chromosomes in human male fibroblast nuclei and prometaphase rosettes. *PLoS Biol.* **3**, e157.

Cavalcanti, A. R., Stover, N. A., Orecchia, L., Doak, T. G. and Landweber, L. F. (2004). Coding properties of *Oxytricha trifallax* (*Sterkiella histriomuscorum*) macronuclear chromosomes: analysis of a pilot genome project. *Chromosoma* **113**, 69-76.

Cook, P. R. (1999). The organization of replication and transcription. *Science* **284**, 1790-1795.

Cremer, T. and Cremer, C. (2001). Chromosome territories, nuclear architecture and gene regulation in mammalian cells. *Nat. Rev. Genet.* **2**, 292-301.

Cremer, T., Kupper, K., Dietzel, S. and Fakan, S. (2004). Higher order chromatin architecture in the cell nucleus: on the way from structure to function. *Biol. Cell* **96**, 555-567.

Erwin, D. H. and Davidson, E. H. (2002). The last common bilaterian ancestor. *Development* **129**, 3021-3032.

Evenson, D. P. and Prescott, D. M. (1970). Disruption of DNA synthesis in *Euplotes* by heat shock. *Exp. Cell Res.* **63**, 245-252.

Fakan, S. and Van Driel, R. (2004). Where do we go in the nucleus? *Biol. Cell* **96**, 553-554.
Gasser, S. M. (2002). Visualizing chromatin dynamics in interphase nuclei. *Science* **296**, 1412-1416.
Grivell, A. R. and Jackson, J. F. (1968). Thymidine kinase: evidence for its absence from *Neurospora crassa* and some other micro-organisms, and the relevance of this to the specific labelling of deoxyribonucleic acid. *J. Gen. Microbiol.* **54**, 307-317.
Gulbis, J. M., Kelman, Z., Hurwitz, J., O'Donnell, M. and Kuriyan, J. (1996). Structure of the C-terminal region of p21(WAF1/CIP1) complexed with human PCNA. *Cell* **87**, 297-306.
Habermann, F. A., Cremer, M., Walter, J., Kreth, G., von Hase, J., Bauer, K., Wienberg, J., Cremer, C., Cremer, T. and Solovei, I. (2001). Arrangements of macro- and microchromosomes in chicken cells. *Chromosome Res.* **9**, 569-584.
Hodson, J. A., Bailis, J. M. and Forsburg, S. L. (2003). Efficient labeling of fission yeast *Schizosaccharomyces pombe* with thymidine and BUDr *Nucleic Acids Res.* **31**, e134.
Hozak, P., Jackson, D. A. and Cook, P. R. (1994). Replication factories and nuclear bodies: the ultrastructural characterization of replication sites during the cell cycle. *J. Cell Sci.* **107**, 2191-2202.
Jaunin, F. and Fakan, S. (2002). DNA replication and nuclear architecture. *J. Cell Biochem.* **85**, 1-9.
Jaunin, F., Visser, A. E., Cmarko, D., Aten, J. A. and Fakan, S. (2000). Fine structural in situ analysis of nascent DNA movement following DNA replication. *Exp. Cell Res.* **260**, 313-323.
Javaux, E. J., Knoll, A. H. and Walter, M. (2003). Recognizing and interpreting the fossils of early eukaryotes. *Origins Life Evol. B* **33**, 75-94.
Jonsson, F. A. L. H. J. (2002). The Biology of Telomeres in Hypotrichous Ciliates. In *Telomerases, Telomeres and Cancer* (ed. G. K. A. R. Parwaresch), pp. 205-222. Georgetown: Landes Bioscience, Kluwer Academic/Plenum Publishers.
Jonsson, F., Postberg, J., Schaffitzel, C. and Lipps, H. J. (2002). Organization of the macronuclear gene-sized pieces of stichotrichous ciliates into a higher order structure *via* telomere-matrix interactions. *Chromosome Res.* **10**, 445-453.
Juranek, S., Jönsson, F., Maercker, C. and Lipps, H. J. (2000). The telomeres of replicating macronuclear DNA molecules of the ciliate *Stylonychia lemnae*. *Protistology* **1**, 148-151.
Kloetzel, J. A. (1970). Compartmentalization of the developing macronuclei following conjugation in *Stylonychia* and *Euplotes*. *J. Cell Biol.* **47**, 395-407.
Kraut, H., Lipps, H. J. and Prescott, D. M. (1986). The genome of hypotrichous ciliates. *Int. Rev. Cytol.* **99**, 1-28.
Krishna, T. S., Kong, X. P., Gary, S., Burgers, P. M. and Kuriyan, J. (1994). Crystal structure of the eukaryotic DNA polymerase processivity factor PCNA. *Cell* **79**, 1233-1243.
Leonhardt, H., Rahn, H. P., Weinzierl, P., Sporbert, A., Cremer, T., Zink, D. and Cardoso, M. C. (2000). Dynamics of DNA replication factories in living cells. *J. Cell Biol.* **149**, 271-280.
Lin, M. and Prescott, D. M. (1985). Electron microscope autoradiography of DNA synthesis in the replication band of two hypotrichous ciliates. *J. Protozool.* **32**, 144-149.
Lipps, H. J. (1980). In vitro aggregation of the gene-sized DNA molecules of the ciliate *Stylonychia mytilus*. *Proc. Natl. Acad. Sci. USA* **77**, 4104-4107.
Lipps, H. J., Nock, A., Riewe, M. and Steinbruck, G. (1978). Chromatin structure in the macronucleus of the ciliate *Stylonychia mytilus*. *Nucleic Acids Res.* **5**, 4699-4709.
Lipps, H. J., Gruissem, W. and Prescott, D. M. (1982). Higher order DNA structure in macronuclear chromatin of the hypotrichous ciliate *Oxytricha nova*. *Proc. Natl. Acad. Sci. USA* **79**, 2495-2499.
Mayr, C., Jasencakova, Z., Meister, A., Schubert, I. and Zink, D. (2003). Comparative analysis of the functional genome architecture of animal and plant cell nuclei. *Chromosome Res.* **11**, 471-484.
Meyer, G. F. and Lipps, H. J. (1981). The formation of polytene chromosomes during macronuclear development of the hypotrichous ciliate *Stylonychia mytilus*. *Chromosoma* **82**, 309-314.
Mollenbeck, M., Postberg, J., Paeschke, K., Rossbach, M., Jonsson, F. and Lipps, H. J. (2003). The telomerase-associated protein p43 is involved in anchoring telomerase in the nucleus. *J. Cell Sci.* **116**, 1757-1761.
Murti, K. G. (1973). Electron-microscopic observations on the macronuclear development of *Stylonychia mytilus* and *Tetrahymena pyriformis* (Ciliophora-Protozoa). *J. Cell Sci.* **13**, 479-509.
Murti, K. G. and Prescott, D. M. (1983). Replication forms of the gene-sized DNA molecules of hypotrichous ciliates. *Mol. Cell Biol.* **3**, 1562-1566.
Murti, K. G. and Prescott, D. M. (2002). Topological organization of DNA molecules in the macronucleus of hypotrichous ciliated protozoa. *Chromosome Res.* **10**, 165-173.
Nakamura, H., Morita, T. and Sato, C. (1986). Structural organizations of replicon domains during DNA synthetic phase in the mammalian nucleus. *Exp. Cell Res.* **165**, 291-297.
O'Keefe, R. T., Henderson, S. C. and Spector, D. L. (1992). Dynamic organization of DNA replication in mammalian cell nuclei: spatially and temporally defined replication of chromosome-specific alpha-satellite DNA sequences. *J. Cell Biol.* **116**, 1095-1110.
Olins, A. L., Olins, D. E., Franke, W. W., Lipps, H. J. and Prescott, D. M. (1981). Stereo-electron microscopy of nuclear structure and replication in ciliated protozoa (Hypotricha). *Eur. J. Cell Biol.* **25**, 120-130.
Olins, D. E. and Olins, A. L. (1994). The replication band of ciliated protozoa. *Int. Rev. Cytol.* **153**, 137-170.
Olins, D. E., Olins, A. L., Cacheiro, L. H. and Tan, E. M. (1989). Proliferating cell nuclear antigen/cyclin in the ciliate *Euplotes eurystomus*: localization in the replication band and in micronuclei. *J. Cell Biol.* **109**, 1399-1410.
Pasero, P., Duncker, B. P. and Gasser, S. M. (1999). In vitro DNA replication in yeast nuclear extracts. *Methods* **18**, 323, 368-376.
Postberg, J., Juranek, S. A., Feiler, S., Kortwig, H., Jönsson, F. and Lipps, H. J. (2001). Association of the telomere-telomere binding protein-complex of hypotrichous ciliates with the nuclear matrix and dissociation during replication. *J. Cell Sci.* **114**, 1861-1866.
Prescott, D. M. (1994). The DNA of ciliated protozoa. *Microbiol. Rev.* **58**, 233-267.
Prescott, D. M. and Kimball, R. F. (1961). Relation between RNA, DNA, and protein syntheses in the replicating nucleus of *Euplotes*. *Proc. Natl. Acad. Sci. USA* **47**, 686-693.
Roth, L. E. (1957). An electron microscope study of the cytology of the protozoan *Euplotes patella*. *J. Biophys. Biochem. Cytol.* **3**, 985-1000.
Sadoni, N., Langer, S., Fauth, C., Bernardi, G., Cremer, T., Turner, B. M. and Zink, D. (1999). Nuclear organization of mammalian genomes. Polar chromosome territories build up functionally distinct higher order compartments. *J. Cell Biol.* **146**, 1211-1226.
Sadoni, N., Cardoso, M. C., Stelzer, E. H., Leonhardt, H. and Zink, D. (2004). Stable chromosomal units determine the spatial and temporal organization of DNA replication. *J. Cell Sci.* **117**, 5353-5365.
Schaffitzel, C., Berger, I., Postberg, J., Hanes, J., Lipps, H. J. and Pluckthun, A. (2001). In vitro generated antibodies specific for telomeric guanine-quadruplex DNA react with *Stylonychia lemnae* macronuclei. *Proc. Natl. Acad. Sci. USA* **98**, 8572-8577.
Schurtenberger, P., Egelhaaf, S. U., Hindges, R., Maga, G., Jonsson, Z. O., May, R. P., Glatter, O. and Hubscher, U. (1998). The solution structure of functionally active human proliferating cell nuclear antigen determined by small-angle neutron scattering. *J. Mol. Biol.* **275**, 123-132.
Sporbert, A., Gahl, A., Ankerhold, R., Leonhardt, H. and Cardoso, M. C. (2002). DNA polymerase clamp shows little turnover at established replication sites but sequential de novo assembly at adjacent origin clusters. *Mol. Cell* **10**, 1355-1365.
Stambrook, P. J. and Flickinger, R. A. (1970). Changes in chromosomal DNA replication patterns in developing frog embryos. *J. Exp. Zool.* **174**, 101-113.
Stein, F. (1859). Der Organismus der Infusionsthiere nach eigenen Forschungen in systematischer Reihenfolge bearbeitet. *Leipzig*: *Engelmann.*
Wray, C. G., Langer, M. R., DeSalle, R., Lee, J. J. and Lipps, J. H. (1995). Origin of the foraminifera. *Proc. Natl. Acad. Sci. USA* **92**, 3075.